

AD-A047 939

NORTH CAROLINA STATE UNIV RALEIGH DEPT OF MATERIALS --ETC F/G 11/2  
MICROSTRUCTURE, ELECTRONIC PROPERTIES AND CHEMICAL DURABILITY 0--ETC(U)  
JUN 77 A A FAHMY

UNCLASSIFIED

ARO-12954.1-MS

DAH04-75-G-0071

NL

[OF]  
ADA047939



AD A 047939

ARO 12954.1-MS

12

MICROSTRUCTURE, ELECTRONIC PROPERTIES AND CHEMICAL DURABILITY  
OF VANADIUM PENTOXIDE-BASED GLASSES AND GLASS-CERAMICS

Final Report

by

Abdel A. Fahmy

June 1, 1977

U. S. ARMY RESEARCH OFFICE

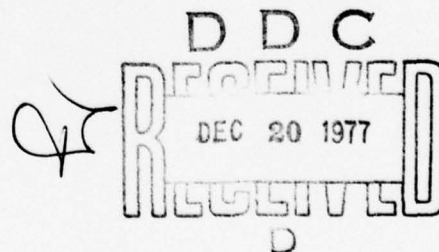
Grant Number DAHC04-75-G-0071

North Carolina State University

Materials Engineering Department

Approved For Public Release  
Distribution Unlimited

The Findings In This Report Are Not To Be  
Construed As An Official Department Of  
The Army Position, Unless So Designated  
By Other Authorized Documents.



AD No. \_\_\_\_\_  
DDC FILE COPY

Unclassified

SECURITY CLASSIFICATION OF THIS PAGE (When Data Entered)

REPORT DOCUMENTATION PAGE		READ INSTRUCTIONS BEFORE COMPLETING FORM
1. REPORT NUMBER DAHCO4-75-G-0071	2. GOVT ACCESSION NO.	3. RECIPIENT'S CATALOG NUMBER
4. TITLE (and Subtitle) Microstructure, Electronic Properties and Chemical Durability of Vanadium-Pentoxide-Based Glasses and Glass-Ceramics.		5. TYPE OF REPORT & PERIOD COVERED Final. 11/1/74 - 4/30/77
7. AUTHOR(s) Professor Abdel A. Fahmy		6. PERFORMING ORG. REPORT NUMBER
9. PERFORMING ORGANIZATION NAME AND ADDRESS North Carolina State University Materials Engineering Department Page Hall, Raleigh, N.C. 27607		8. CONTRACT OR GRANT NUMBER(s) ✓ DAHCO4-75-G-0071 new
11. CONTROLLING OFFICE NAME AND ADDRESS U. S. Army Research Office Post Office Box 12211 Research Triangle Park, N.C. 27709		10. PROGRAM ELEMENT, PROJECT, TASK AREA & WORK UNIT NUMBERS R & D Project No and Title: 1T161102B32D Intrinsic Studies of Materials
14. MONITORING AGENCY NAME & ADDRESS (if different from Controlling Office) Final rept. 1 Nov 74 - 30 Apr 77		12. REPORT DATE 6-1-77
16. DISTRIBUTION STATEMENT (of this Report) Approved for public release, distribution unlimited 12 43p.		13. NUMBER OF PAGES 31
17. DISTRIBUTION STATEMENT (of the abstract entered in Block 20, if different from Report) NA 18 ARO 19 12954.1-MS		15. SECURITY CLASS. (of this report) Unclassified
15a. DECLASSIFICATION/DOWNGRADING SCHEDULE		
18. SUPPLEMENTARY NOTES The Findings in this report are not to be construed as an official Department of the Army position, unless so designated by other authorized documents.		
19. KEY WORDS (Continue on reverse side if necessary and identify by block number) Glass, Glass-ceramics, Vanadium Pentoxide, Electronic Conductivity, Magnetic Susceptibility, Chemical Durability.		
20. ABSTRACT (Continue on reverse side if necessary and identify by block number) Crystallization of Vanadium Pentoxide from Vanadium Pentoxide-Phosphorous Pentoxide glasses containing 0-9 mol% Boron Trioxide during heat treatment in the range 220°C-410°C caused progressive microstructural changes which dramatically affected the electronic conductivity, the activation energy for conduction, and the resistance to chemical attack. All compositions were approximately 83% crystalline after heating to 410°C. As a result, the values of conductivity and activation energy were almost identical to those observed for pure polycrystalline Vanadium-Pentoxide.		

DD FORM 1 JAN 73 1473 EDITION OF 1 NOV 65 IS OBSOLETE

Unclassified

SECURITY CLASSIFICATION OF THIS PAGE (When Data Entered)

408 886

LPB

#### Additional Final Reporting Requirements

1. Statement of Problem - See page 2 of report.
2. Summary of Important Results - See page 20 of report.
3. List of Publications:
  - a) Y. Limb, K. Y. Cheng, J. C. Hurt and R. F. Davis, in Sixth International Materials Symposium, Ceramics Microstructures - '76, Berkeley, California, Aug. 1976, to be published.
4. Participating Scientific Personnel:
  - a) Abdel A. Fahmy
  - b) Young Limb - Earned Ph.D. degree 5/77, North Carolina State University.

ACCESSION NO.	
NTIS	Write Section <input checked="" type="checkbox"/>
DOC	Self Section <input type="checkbox"/>
UNANNOUNCED	<input type="checkbox"/>
JUSTIFICATION	
BY	
DISTRIBUTION/AVAILABILITY CODES	
Dist.	AVAIL. and/or SPECIAL
A	



## TABLE OF CONTENTS

<u>Topic</u>	<u>page</u>
I. Introduction	1
II. Experimental Procedure	4
III. Results and Discussion	8
A. Microstructure	8
B. Conductivity	12
C. Chemical Durability	18
IV. Conclusions	20
V. Bibliography	21

### Figure Captions

Figure 1. (A) typical DTA curve and (B) resulting heat treatment schedule for all  $V_2O_5$ -based glasses of this research. The separate  $220^\circ\text{C} - 4$  hrs. anneal is not shown in (B); the  $235^\circ\text{C}$  temperature was found necessary to allow some initial structural readjustment in the glasses prior to the onset of crystallization.

Figure 2. Replicate TEM micrographs showing progressive phase separation and crystallization in the 000 glass. (A) as cooled, (B)  $220^\circ\text{C} - 4$  hrs., (C)  $290^\circ\text{C} - 6$  hrs and (D)  $410^\circ\text{C} - 6$  hrs. (bar =  $0.5\mu\text{m}$ )

Figure 3. Replicate TEM micrographs, representative of all ternary compositions, showing crystallization in the 006 glass. (A)  $290^\circ\text{C} - 6$  hrs. and (B)  $410^\circ\text{C} - 6$  hrs. The microstructure of the as-cooled and annealed glasses are similar to those of Fig. 2(A),(B). (bar =  $0.5\mu\text{m}$ )

Figure 4. SEM micrographs showing the polycrystalline  $V_2O_5$  in polished and etched surfaces of (A), (B) 000- $290^\circ\text{C} - 6$  hrs., (C) 000 -  $410^\circ\text{C} - 6$  hrs., (D) 006 -  $290^\circ\text{C} - 6$  hrs. and (E) 006- $410^\circ\text{C} - 6$  hrs. (D) and (E) are representative for all analogous ternary samples. (A) was etched with  $\text{H}_2\text{O}$  for 90 sec; all others etched with 1%  $\text{HCl}$  for 50 sec, (bar =  $1\mu\text{m}$ )

Figure 5. Curves of  $\log \sigma T$  vs.  $1/T$  showing the changes in conductivity as a function of the temperature of crystallization for compositions (A) 000 and (B) 006, respectively, and as a

function (C) of the changing  $V_2O_5$  content in the glasses annealed at 220°C.

Figure 6. Curves of percentage weight loss of the annealed and progressively crystallized glasses as a function of the log of time of immersion in static  $H_2O$ .

MICROSTRUCTURE, ELECTRONIC PROPERTIES AND CHEMICAL DURABILITY  
OF  $V_2O_5$ -BASED GLASSES AND GLASS-CERAMICS

BY

Abdel A. Fahmy

I. INTRODUCTION

Vanadium pentoxide is oxygen deficient when nonstoichiometric; the extra electrons are localized at  $V^{5+}$  centers resulting in the formation of reduced vanadium ions, normally  $V^{4+}$ . Furthermore, these electrons remain in the vicinity of these centers for a time longer than the average lattice vibration period; thus, the atoms in the neighborhood of the excess charge have sufficient time to assume new equilibrium positions consistent with the presence of the added charge. These displacements produce a potential well for the excess electrons such that they occupy a bound state, being unable to move without a change in the positions of the surrounding atoms. A bound electron and its associated lattice deformation are termed a polaron. A small polaron, the principal charge carrier in  $V_2O_5$ -based glasses, implies that the self-trapped carrier is essentially confined to a "small region", typically a single atomic site. Electronic conduction in  $V_2O_5$ -based glasses at  $T > 1/2\theta_D$  ( $\theta_D$ =Debye temperature) is believed to occur by the thermally activated hopping of small polarons between vanadium sites.



The present level of understanding of the conduction process in  $V_2O_5$ -based glasses has been derived by the numerous theoretical and experimental efforts generated since the research of Stanworth and co-workers<sup>1,2</sup>. Contemporary reviews of this research have been published by Mackenzie<sup>3a,b</sup>, Austin and Mott<sup>4</sup>, Adler<sup>5</sup>, and Kinser and Wilson<sup>6</sup>.

Investigators have also detected large-scale and microphase separation and/or crystallization in  $V_2O_5$ -based glasses, as reviewed by the present authors.<sup>7</sup> The reports of these two transformations have almost been divorced from one another even though these events are now considered sequential in many glasses which undergo fine-scale bulk crystallization. Only limited information concerning the origin of the amount, size or type of crystallization product has been presented, with the exception of the present research. Hamblet et al.<sup>8</sup> and Hench<sup>9</sup> observed a three order decrease in resistivity upon heating a  $67V_2O_5-33KPO_3$  glass at 288° and 310°C, respectively. Even though the temperature difference was small, the former author observed inhomogeneous formation of large crystals (supposedly on the surface) while the latter writer found less than 0.1% bulk crystallinity. Heterogeneous large-scale liquid immiscibility has also been reported by Jamakirama-Rao<sup>10</sup> in optical microscope studies of  $V_2O_5-P_2O_5-B_2O_3$  glasses containing considerable  $B_2O_3$ .

The objectives of the research reported herein were to correlate the changes in microstructure which occurred in the  $V_2O_5-P_2O_5$  and  $V_2O_5-P_2O_5-B_2O_3$  glasses as a result of heat treatment with 1) the changes in electronic conductivity and other related physical properties and

2) the solubilities of these resultant materials in  $H_2O$  as a function of time.

$B_2O_3$  was initially added to the binary system because of 1) the difficulty experienced by several authors<sup>8,9,11</sup> in producing homogeneous fine-grained glass-ceramics containing a near maximum percentage of crystalline  $V_2O_5$  and 2) the authors' reasoning that any  $B_2O_3$  in four-fold coordination would probably be compatible with the  $PO_4$  structure but not with the  $VO_5$  quasi-trigonal bipyramidal structure thought to exist in these types of glasses. It was surmised that the  $BO_4-PO_4$  combination would enhance the incompatibility of the  $V_2O_5$  and cause it to become unstable to crystallization. It was later found that the binary could also be crystallized but with a different microstructure. The original reasoning is not made void, however, as the velocity of the crystallization of the ternary materials is considerably greater than that of the binary, as discussed more fully below.

## II. EXPERIMENTAL PROCEDURE

The glass compositions shown in Table I were prepared by dry-mixing the oxides\* of each component in quantities such that the total of each batch could be incorporated in a covered 100cc platinum crucible. All compositions were melted in air at  $800^{\circ}\pm 5^{\circ}\text{C}$  for one hour, stirred with a fused silica rod, poured into a preheated ( $220^{\circ}\text{C}$ ) cylindrical graphite mold to prevent fracture from thermal shock, annealed at  $220^{\circ}\text{C}$  for 4 hours and allowed to cool with the furnace. Samples were placed in a desiccator to prevent attack by atmospheric moisture. The first three numbers of each sample designation denotes the boron concentration in mol%; the last three numbers (when used) denotes the temperature of heat treatment.

Table I. Composition, Activation Energy for Conduction and Conductivity Pre-exponential Term of the  $\text{V}_2\text{O}_5$ -based glasses and glass ceramics

Sample No.	Composition (mole%)			Activation Energy(eV) and $[\sigma_0 \times 10^{-3}]$		
	$\text{V}_2\text{O}_5$	$\text{P}_2\text{O}_5$	$\text{B}_2\text{O}_3$	$220^{\circ}\text{C}$	$290^{\circ}\text{C}$	$410^{\circ}\text{C}$
000	84	16	0	0.408[22.7]	0.307[11.6]	0.270[ 7.5]
003	84	13	3	0.368[10.0]	0.294[ 8.7]	0.270[ 8.1]
006	81	13	6	0.390[14.8]	0.300[ 7.5]	0.281[10.9]
009	78	13	9	0.438[52.2]	0.300[ 5.8]	0.281[ 8.1]

\*Fisher certified grade  $\text{V}_2\text{O}_5$  and  $\text{P}_2\text{O}_5$ . Lot no. and principal impurities of these components are as follows:  $\text{V}_2\text{O}_5$  (730793)-Fe 0.01%, Cl 0.01%;  $\text{P}_2\text{O}_5$  (791283)-As 0.003%, Pb 0.005%,  $\text{NH}_4$  0.004%;  $\text{B}_2\text{O}_3$  was classified Fisher reagent grade.

To induce subsequent crystallization, all samples used for the conductivity and related studies were positioned on fiberfrax felt in a Kanthal wound furnace controlled within  $\pm 5^\circ\text{C}$  and heated according to the schedule shown in Fig. 1(B). This schedule was derived from the DTA results, Fig. 1(A), determined at a heating rate of  $10^\circ\text{C}/\text{min}$ .

Samples of 003 and 009 annealed at  $220^\circ\text{C}$  as well as 000 and 006 heated at  $220^\circ$ ,  $290^\circ$ , and  $410^\circ\text{C}$  were analyzed by wet chemical analysis\* for  $\text{V}^{5+}$  and  $\text{V}^{4+}$  by standard techniques.<sup>12</sup> The concentration of  $\text{V}^{4+}$  was also determined independently by magnetic susceptibility measurements on all samples of this research. The Faraday method<sup>13</sup> was employed using  $\text{HgCo}(\text{CNS})_4$  as a standard having a known value of unpaired electrons. Densities of all samples were determined by the method of Archimedes. Pure ethanol of a known temperature (accuracy =  $\pm 0.1^\circ\text{C}$ ) was used as the liquid medium.

Microstructural evolution as a function of temperature in each composition was characterized by 1) TEM\*\* using replicas of polished or freshly fractured surfaces etched in distilled water for approximately 20 seconds 2) SEM\*\* of polished surfaces etched in  $\text{H}_2\text{O}$  for 90 sec or 1% aqueous HCL solution for 50 seconds and 3) a determination of the vol% crystallinity by a point counting technique using fifteen  $1'' \times 1''$  grids each having 64 points on a TEM micrograph having magnification of 50,000X.

Finely ground 1.5" dia. by 0.25 thick samples were used for all d.c. and a.c. conductivity measurements. Ohmic contacts for these

---

\* Herron Testing Laboratories, Cleveland, Ohio.

\*\* TEM, JEM-120; SEM JSM-2 and JSM-35.



measurements were produced by applying a thin layer of platinum paste<sup>†</sup> to both sample faces with a camel-hair brush and annealing for 150°C for 2 hours. The effectiveness of this process was demonstrated by a linear I-V curve which passed through zero; furthermore, the a.c. conductivity showed no apparent frequency dependence.

The conductivity of the samples is relatively high ( $>10^{-5} \text{ ohm}^{-1} \text{ cm}^{-1}$ ); thus, a two electrode arrangement was used. In both d.c. and a.c. measurements, the samples were positioned in an Inconel 601\* grounded container. The controlling temperature (accuracy =  $\pm 0.5^\circ\text{C}$ ) was measured at the sample. All lead wires inside the furnace were 0.04" nichrome wire due to the temperature employed. The line resistance of these wires and their copper extensions were measured independently of the sample as a function of temperature and subtracted from the measured values to obtain the data for each sample.

Determination of the d.c. and a.c. conductivities utilized a Hewlitt Packard 34703 multimeter and 34740 display meter coupled to a Keithley recorder for the former measurement and a Hewlitt Packard 4800A vector impedance meter for the latter study. The temperature and frequency ranges employed were 25-400°C and  $10^2 - 10^5$  Hz, respectively. Each sample was measured to within 10° of the maximum temperature (annealing or crystallization) to which it had been previously subjected.

The relative resistance to chemical attack of the various types

---

<sup>†</sup> Engelhard #6926, unfluxed

\* Huntington Alloys, INCO, Inc. Nominal composition in wt, %: 58-63 Ni, 21-25 Cr, remainder Fe.

of samples was determined by measuring the weight loss of a cube 0.635 cm on an edge immersed in 65 cm<sup>3</sup> of static distilled water for varying lengths of time. (Unfractured spherical samples having identical diameters could not be produced). Upon removal from the water, each sample was sprayed with ethanol, dried in air and weighed (accuracy  $\pm 0.1\text{mg}$ ).

Complete descriptions of all the procedures outlined above may be found in Ref. 14.

### III. RESULTS AND DISCUSSION

#### A. Microstructure

Figs. 2(A,B) are representative of the microstructures possessed by both the binary and the three ternary as-cooled and annealed glasses. The unannealed glasses, Fig. 2(A), show little evidence of phase separation even at high (100K) magnification whereas, the annealed materials, Fig. 2(B), contain a distinct second phase of homogeneously nucleated tiny  $V_2O_5$ -rich droplets. Increasing the temperature further immediately results in the enhanced coalescence of the droplet phase with the initial vestiges of crystallization of  $V_2O_5$  occurring at approximately 250°C. The latter phenomenon reaches an initial maximum at approximately 290°C, Figs. 2(C) & 3(A).

Following the 290°C crystallization, the microstructures of the three ternary compositions are also similar but are notably different from that of the analogous binary materials. This is particularly evident in the SEM micrographs, Figs 4(A,B,D). In the 290°C binary materials, the irregular-shaped submicron  $V_2O_5$  crystals form clusters which appear to be in loose contact with each other at a few points but are primarily bounded by the residual glass phase. This is most clearly evident in the lightly etched samples, Fig. 4(A). The existence of a rim of glass of varying thickness surrounding portions of a few of the individual grains is also seen at higher magnifications of the same sample; however, most of the grains appear to maintain large areas of contact with each other within a particular cluster. As such, a more severe etch, Fig. 4(B), causes considerable undermining and removal of whole clusters of grains during the reaction, which is also evident in the chemical durability studies.

The addition of  $B_2O_3$  in the amounts shown in Table I produces an increasingly more rigid glass as a direct function of the concentration of this compound. Unlike the binary material, the ternary samples must be carefully heated to  $290^\circ C$  in order to produce a crack-free crystallized sample even though the bulk density changes are less in the latter materials. Indeed a crack-free sample containing 12 mol%  $B_2O_3$  could not be produced. Furthermore NMR analysis of the  $^{11}B$  nucleus<sup>7</sup> reveals considerable distortion in the  $BO_4$  tetrahedra in all samples except those heated at  $410^\circ C$  - a further indication of the stresses in the ternary materials which exists even after the initial crystallization.

As a result of the addition of  $B_2O_3$ , the microstructures of the ternary samples at  $290^\circ C$ , Fig. 4 (D), possess unclustered, apparently interlocking, rod-shaped crystals which are larger than those of the binary material and again have at least a loose point contact with each other. The residual glass appears to encompass a portion of each crystal as well as form spherical "nodules" at selected sites throughout the microstructure, Fig. 3(A).

In an earlier report<sup>7</sup> on the ternary materials, it was noted that 1) the intensity of the DTA peak at  $410^\circ C$  was directly proportional to the boron content and 2) the heat treatment at  $410^\circ C$  considerably enhanced the chemical durability of these materials. These phenomena were formerly attributed to the formation of an amorphous  $BPO_4$  phase initially postulated by Kreidl and Weyl<sup>15</sup> to explain the chemical durability of alkali-modified borophosphate glasses. Additional evidence for the presence of  $BPO_4$  has also been presented by Takahashi<sup>16</sup> and Ray<sup>17</sup>. Subsequent DTA research on 1) the binary glass and 2) a glass



having the calculated composition of the amorphous matrix of the 006-290°C material of this research has revealed the exothermic reaction at 410°C in both compositions, and it is now attributed to the second crystallization of  $V_2O_5$ . This second, high temperature formation of  $V_2O_5$ , Figs. 2(D) & 3(B) is also to be expected from the compositions of the residual glasses as shown by the studies of Nador<sup>18</sup> and Anderson and Compton<sup>19</sup>. The  $BPO_4$  phase is however, believed to be a possibility, forming at lower temperatures or during cooling from the melt and contributing to the durability, the rigidity and the amount of  $V_2O_5$  at 410°C.

This additional crystallization of  $V_2O_5$  at 410°C in the binary is also reflected in the SEM microstructure, Fig. 4(C), in that the crystal clusters are now larger and bond to each other more extensively than at 290°C. Furthermore, glass between the individual grains is no longer evident at higher magnifications.

In the ternary samples, increased diffusion rates cause the 410°C crystallization, Fig. 4(E), to be preceeded or accompanied by a rounding of the rod-like crystals and an increase in the interfacial area of contact between the grains. As a consequence of these effects much of the glass is isolated in pockets throughout the samples. The decreased viscosity of the samples evident in the stress removal shown in the NMR results may also contribute to the greater interfacial area through particle rearrangement.

As already noted or implied, the progressive evolution of the above microstructures also affected changes in the percent crystallinity and bulk density as shown in Table II. An examination of this table shows

that the amount of crystalline  $V_2O_5$  at 290°C and 410°C, respectively, is very nearly the same in all compositions. There is a 7-8 wt% increase in  $V_2O_5$  at 410°C in all compositions which is reflected in the increase in the bulk density of these samples. The ratio of the crystalline  $V_2O_5$  to that contained in the original batch composition increased with an increase in boron content and is nearly unity for the 009 composition. This possibly reflects the ability of  $B_2O_3$  to force  $V_2O_5$  out of solution, as discussed in the introduction. These changes in the microstructure, percent crystallinity and density notably affect the electronic conductivity and chemical durability as discussed below.

Table II. Percent  $V_2O_5$  Crystallinity\* and Bulk Density of  $V_2O_5$ - $P_2O_5$ - $B_2O_3$  Glasses

Sample No.	$V_2O_5$ (wt%) Batch Comp.	Crystallinity (wt%)		Bulk Density (g/cc)					
		290°C	410°C	220°C	Δ%	290°C	Δ%	410°C	
000	87	75	82	2.830	9.65	3.103	1.61	3.153	
003	88	75	83	2.945	6.04	3.123	1.50	3.170	
006	87	77	84	2.914	5.73	3.081	1.91	3.140	
009	85	76	84	2.888	7.49	3.047	2.13	3.112	

\*Values reported previously<sup>7</sup> were determined by x-ray diffraction counting techniques. The values given above and determined as noted in the experimental procedure are considered more accurate.

## B. Conductivity

Plots of  $\log \sigma T$  vs.  $1/T$  were found to be linear regardless of heat treatment temperature or composition. Figs. 5(A,B) are representative of the changes in d.c. conductivity and activation energy which accompany the progressive crystallization of the annealed phase-separated glasses. The latter values as well as  $\sigma_0$  calculated from these plots are given in Table I.

Theoretical and experimental research<sup>(4,20)</sup> concerned with the polaron hopping process has lead to an expression for the d.c. conductivity,  $\sigma$ , of the form,

$$\sigma = \frac{k c(1-c)}{T} \exp\left(-\frac{W}{KT}\right) \quad (1)$$

where  $k$  is a constant, and  $c$  and  $(1-c)$  are the  $V^{4+}/V^{\text{total}}$  and  $V^{5+}/V^{\text{total}}$  ratios, respectively, and  $W$  is the activation energy for conduction.

These ratios in the present research were determined from two independent measurements; wet chemical analysis and magnetic susceptibility. The results of these measurements are presented in Table III for selected heat treatment temperatures.

The derived values of  $c$  indicate that the concentration of  $V^{4+}$  is essentially independent of temperature of heat treatment and composition. The former relationship was also found by Lynch et al.<sup>21</sup> at various temperatures in the range 77°-330°K and by Mackenzie and coworkers<sup>22</sup> between 20° and 350°C using ESR and Seebeck coefficient measurements<sup>5</sup>, respectively. This relationship shows that the temperature dependence of the conductivity arises from changes in the effective carrier mobility. The absence of any temperature dependence of  $c$  over the range from room temperature to 410°C indicates that the average site symmetry of the positions occupied by electrons is unchanged within experimental error.

Landsberger and Bray<sup>23</sup> have presented NMR evidence that the vanadium ions in the glass are five-fold coordinated as in crystalline  $V_2O_5$ . This conclusion has also been reached in infrared<sup>19</sup> and ESR<sup>24</sup> research. It is also important to note that ESCA analysis<sup>\*</sup> of the 006 glass and glass-ceramics during the course of this research revealed no  $V^{3+}$  in these materials.

Table III.  $V^{4+}$ ,  $V^{5+}$ , and c as determined from Wet Chemical Analysis and Magnetic Susceptibility Measurements.

Sample No.	$V^{4+}$ (wt.%) <sup>*</sup>	$V^{5+}$ (wt.%) <sup>*</sup>	$c^* \times 10^2$	$c^{**} \times 10^2$
000-220	4.38	43.88	9.1	9.2
000-290	4.24	44.85	8.6	9.0
000-410	4.77	43.92	9.8	9.5
003-220	3.47	45.04	7.2	7.1
003-290				7.1
003-410				6.8
006-220	3.68	44.09	7.7	9.3
006-290	3.54	44.17	7.4	9.3
006-410	3.01	44.55	6.3	9.6
009-220	3.22	45.16	6.7	8.3
009-410				9.0

\* Wet chemical analysis

\*\* Magnetic susceptibility; no diamagnetic correction was made as the data for  $V^{5+}$  is not available.

\* Physical Electronics, Inc., Eden Prairie, Minn.



As a result of the constancy of  $c$ , the equation for  $\sigma$  may be written

$$\sigma = \frac{\sigma_0}{T} \exp\left(-\frac{W}{KT}\right) \quad (2)$$

where  $\sigma_0 = k c(1-c) = \text{constant}$ . This is in general agreement with the experimental results of the crystallized materials shown in Table I and Fig. 5. The precise reason(s) for the higher values of  $\sigma_0$  in 000 and 009-220 is not known at this time.

A synthesis of the foregoing results with the polaron model indicates that the change in conductivity which is induced by heat treatment must be solely explained by the variation of  $W$ . Table I shows that the value of  $W$  progressively decreases with heat treatment, thus increasing the conductivity of the sample.

According to Austin and Mott<sup>4</sup>, the activation energy for conduction is given by  $W = W_H + 1/2W_D$  where  $W_H$  and  $W_D$  are the polaron hopping energy and the activation energy for hopping due to disorder, respectively. In vanadate glasses,  $W_D$  is negligible relative to  $W_H$ , except at low temperatures.<sup>4,25</sup> If two ion centers are near each other such that their polarization clouds overlap, the value of  $W_H$  is decreased by the amount<sup>4</sup>

$$W_H = \frac{e^2}{4\pi K_p} \left( \frac{1}{r_p} - \frac{1}{R} \right) \quad (3)$$

where  $K_p$ ,  $r_p$  and  $R$  are the effective dielectric constant, the polaron radius and average hopping distance, respectively.

From the batch compositions and density values, the authors have calculated  $R$  for the annealed ternary glasses to be 3.89 Å (003), 3.91 Å (006), and 3.94 Å (009), respectively. Substitution of the above

values of  $R$  into Eq.(3), however, gives a much smaller range of values for  $W$  than actually measured, Fig. 5(C). This is believed to be attributed to the fact that the calculated values of  $R$  are based on the assumption of complete homogeneity in the glasses; whereas, in reality the latter are phase separated into  $V_2O_5$ -rich amorphous droplets surrounded by a matrix glass which controls the value of  $W$  and is deficient in  $V_2O_5$  relative to the initial batch composition. To explain the rather large variation in activation energy with composition, the authors believe that increasing the  $B_2O_3$  content enhances the incompatibility between the V-O units and the parent glass. This results in a notable decrease in the  $V_2O_5$  concentration and more rapid increases in the vanadium ion separation and thus the activation energy for conduction in the continuous matrix glass than would occur in a homogeneous glass. This effect on  $W$  is in addition to that caused by the simple replacement of  $V_2O_5$  by  $B_2O_3$  in the batch composition.

Separate plots similar to 5(C) for all the 290°C and the 410°C crystallized samples reveal essentially overlapping linear curves for each temperature.

The formation of the highly-conducting  $V_2O_5$  polycrystalline phase at 290°C provides the principal conduction path for electrons and results in a considerable decrease in the activation energy and a concomitant increase in the conductivity at this temperature. Although it cannot be determined conclusively from Figs. 4(A) & (D) or supplementary micrographs whether or not the crystals and crystal clusters are in direct contact with each other; conductivity measurements on the calculated residual glass compositions have values in the range of  $10^{-8} \text{ ohm}^{-1} \text{ cm}^{-1}$ . A glass rim surrounding each grain would control

conductivity; however, the actual values of  $\sigma$  and  $W$  are much closer to that of the pure material than those of the measured glass. It can thus be postulated that the crystals and crystal clusters share at least a loose point contact with each other.

A second point of view is also relevant. As much of the residual glass congregates in large islands in the microstructure (see, e.g., Figs. 3(A) & 4(A)), it is also possible that a very thin rim of glass does exist between points of closest approach of the crystals and that the 6 hr. heating time allows diffusion of some V-O species from the crystals into this glass, thus establishing a higher than average concentration of vanadium ions between the crystals and increasing the conductivity.

The diffusion noted above would be enhanced by an increase in temperature and would thus explain the ease of additional crystallization evident in all samples at 410°C and the considerable rounding of the rod-shaped particles seen in the ternary 410°C micrographs, Fig. 4(D). These resultant phenomena allow much better grain and cluster contact and enlarge the resultant interfacial areas of these contacts.

As a result of the additional crystallization and structural rearrangement,  $\sigma$  and  $W$  (calculated from  $\sigma = \sigma_0 \exp(-W/kT)$  to facilitate comparison) at 25°C for all the 410°C samples averaged  $5.96 \times 10^{-4} \text{ ohm}^{-1} \text{ cm}^{-1}$  and 0.239 eV respectively, which are very close to the  $6.31 \times 10^{-4} \text{ ohm}^{-1} \text{ cm}^{-1}$  and 0.23 eV observed for pure polycrystalline  $\text{V}_2\text{O}_5$ .<sup>26</sup>

In summary, when the glasses are heated at 290°C or 410°C, the conducting medium becomes the  $V_2O_5$  crystals, the average hopping distance is decreased and  $W$  becomes essentially independent of  $B_2O_3$  concentration as shown in Table I.

The values of a.c. conductivity in all samples were equal to those determined in the d.c. measurements and no apparent frequency dependence was observed. This is in agreement with the work in this temperature range of other investigations. 5,25,27



### C. Chemical Durability

A major barrier to the commercial utilization of glasses having compositions similar to the ones of this research is their considerable susceptibility to attack by an  $H_2O$ -containing environment, due principally to the presence of  $P_2O_5$ .

The rate of chemical attack of the glasses annealed at  $220^\circ C$  was approximately the same for all compositions; however, the resistance of the crystallized samples revealed a definite dependency on heat treatment temperatures and boron content, as shown in Figs. 6(A-C). The increase in chemical durability following crystallization at  $290^\circ C$  for all compositions relative to that of the respective glasses must be ascribed principally to the microstructure. All ternary samples produced at this temperature were approximately equal in durability but much more durable than the analogous binary material. This may be explained by the changes in microstructure which occurred during the reaction, as noted above. The  $H_2O$  etches away primarily the residual glass in the ternary samples; whereas, whole or parts of clusters of crystals may also be removed with the glass in the binary material. In addition the interlocking nature of the crystals in the ternary materials may act to retard the rate of chemical attack.

Following the heat treatment at  $410^\circ C$ , the binary sample has a considerably improved durability to attack due to the additional crystallization between the clusters as well as the individual grains. This allows greater attachment between the clusters and prevents their removal during the etch.

The analogous ternary materials are not only less soluble than the binary specimen but show a further reduction in solubility as a direct function of increased boron content. The former phenomenon is due principally to the much larger and continuous interfacial contact between the individual grains, the lack of grain clustering and the isolation of much of the glass into pockets throughout the bulk.

Those microstructural changes in the ternary materials may also be coupled with the formation of a small amount of the aforementioned  $\text{BPO}_4$  phase whose concentration increases with the increase in  $\text{B}_2\text{O}_3$  and causes the differences among the solubilities of the 003, 006 and 009 materials, Fig. 6(C). The elimination of  $\text{V}_2\text{O}_5$  from the amorphous phase at  $290^\circ\text{C}$  and subsequent heating of the residual glass enhances the opportunity for the B and P species to react with each other to form the borophosphate phase. Takahashi<sup>16</sup> has found that  $\text{Na}_2\text{O}-\text{P}_2\text{O}_5-\text{B}_2\text{O}_3$  glasses have excellent durability in the acid regions, i.e., where  $\text{Na}_2\text{O}/\text{P}_2\text{O}_5 < 1$ , and particularly (and more cogent for the present research) in the range where  $\text{B}_2\text{O}_3/\text{P}_2\text{O}_5 < 1$ . Ray<sup>17</sup> has regarded these types of glasses to be linear polyphosphates cross linked by boron in three-and-four-fold coordination, depending on the overall composition. The cross link density of boron, especially in the higher coordination, progressively increases both the transformation temperature and the resistance to water attack. Finally, additional indirect evidence for the formation of this phase lies in the fact that the percent change in bulk density during heating from  $290^\circ\text{C}$  to  $410^\circ\text{C}$  is greater in direct proportion to the  $\text{B}_2\text{O}_3$  concentration. As the initial and final amounts of crystallinity are approximately the same in each composition, this may be an indication of the increased structural tightening of the residual glass phase.

#### IV. CONCLUSIONS

1. Phase separation and subsequent crystallization of  $V_2O_5$  from coalesced amorphous droplets are easily accomplished in  $V_2O_5-P_2O_5$  and  $V_2O_5-P_2O_5-B_2O_3$  glasses by judicious heat treatment at 220°C for the former and 290°C and 410°C for the latter transformation.
2. The d.c. conductivity and the activation energy for conduction dramatically increases and decreases, respectively, with heat treatment of the glasses at both 290°C and 410°C. These changes at both temperatures are primarily attributed to the formation of the continuous and highly conducting polycrystalline vanadium pentoxide phase.
3. The values of  $V^{4+}/V^{total}$  are essentially constant for all compositions and phase assemblages and, thus, are also independent of temperature of heat treatment. The values of  $\sigma_0$  in the crystallized materials are also relatively unchanged; thus, the conductivity in these substances is controlled principally by the changes in activation energy.
4. This progressive crystallization of  $V_2O_5$  also greatly increases the resistance to water attack. The presence of grain clusters partially surrounded by an amorphous phase causes greater weight loss for a given time in the binary than in the ternary sample.

# BIBLIOGRAPHY

1. E. P. Denton, H. Rawson and J. E. Stanworth, *Nature* 173, 1030 (1954).
2. P. L. Baynton, H. Rawson and J. E. Stanworth, *J. Elect. Chem. Soc.* 104, 237 (1957).
- 3a. J. D. Mackenzie, in *Modern Aspects of the Vitreous State* 3, 126 (1964).  
b. J. D. Mackenzie, in *Electrical Conductivity in Ceramics and Glasses*, Part B, N. M. Tallan, ed., Marcel Dekker, Inc., pp. 579-591 (1974).
4. I. G. Austin and N. F. Mott, *Advan. in Physics* 18, 41 (1969).
5. D. Adler, *Critical Reviews of the Solid State* 1, 405 (1970).
6. D. L. Kinser and L. K. Wilson, in *Recent Advances in Science and Technology of Materials*, Vol. 1, A. Bishay, ed., Plenum Press Inc., New York, pp. 77-90 (1974).
7. Y. Limb, K. Y. Cheng, J. C. Hurt and R. F. Davis, in *Sixth International Materials Symposium, Ceramic Microstructures - '76*, Berkeley, California, Aug. 1976, to be published.
8. D. P. Hambley, R. A. Weidel, and G. E. Blair, *H. Am. Cer. Soc.* 48, 499 (1963).
9. L. L. Hench, *J. Noncryst. Solids*, 2, 250 (1970).
10. Bh. D. Janakirama-Rao, in *Frontiers of Glass Science*, Proceed. of the Annual Meeting of the Int. Comm. on Glass (London), p. 17 (1970),
11. A. Mansingh, J. K. Vaid and R. P. Tandon, *J. Phys. C: Solid State Phys.* 8, 1023 (1975).
12. R. M. Brown, Ph. D. thesis, U. of Illinois, Ann Arbor, Michigan (1966).
13. A. Earnshaw. *Introduction to Magnetochemistry*, Academic Press Inc., New York, (1968).
14. Y. Limb, Ph.D. thesis, North Carolina St. U., Raleigh, N.C. (1977).
15. N. Kreidl and W. Weyl, *J. Am. Cer. Soc.* 24, 337 (1941).
16. K. Takahashi in *Advances in Glass Technology: Technical papers of the Sixth International Congress on Glass*, Washington, D.C., Plenum Press Inc., New York, p. 367 (1962).



17. N. H. Ray, Phys and Chem. of Glasses 16, 75 (1975).
18. B. Nador, ~~Glass~~ and Ceramics, 17, 517 (1960).
19. G. W. Anderson and W. D. Compton, J. App. Phys., 52, 6166 (1970).
20. G. S. Linsley, A. E. Owen, and F. M. Hayatee, J. Noncryst. Solids, 4, 208 (1970).
21. G. F. Lynch, M. Sayer, S. L. Segel, and G. Rosenblatt, J. Appl. Phys. 42, 2587 (1971).
22. T. Allersma and J. D. Mackenzie, Jour. Chem. Phys. 47, 1406 (1967).
23. F. R. Landsberger and P. J. Bray, J. Chem. Phys., 53, 7 (1970).
24. E. J. Friebele, L. K. Wilson and D. L. Kinser, J. Am. Cer. Soc. 55, 164 (1972).
25. H. H. Nester and W. D. Kingery, in International Conference on Glass, Brussels, p. 106 (1963).
26. T. Allersma, R. Hakim, T. N. Kennedy and J. D. Mackenzie, J. Chem. Phys., 46, 1 (1970).
27. M. Sayer, A. Mansingh, J. M. Reyes and G. Rosenblatt, J. Appl. Phys. 42, 2857 (1971).

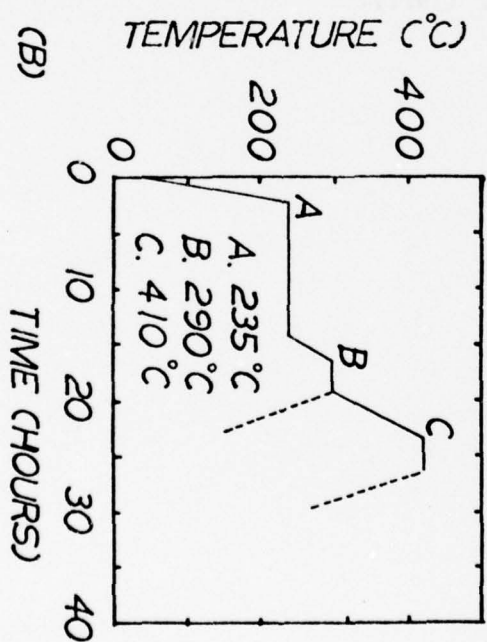
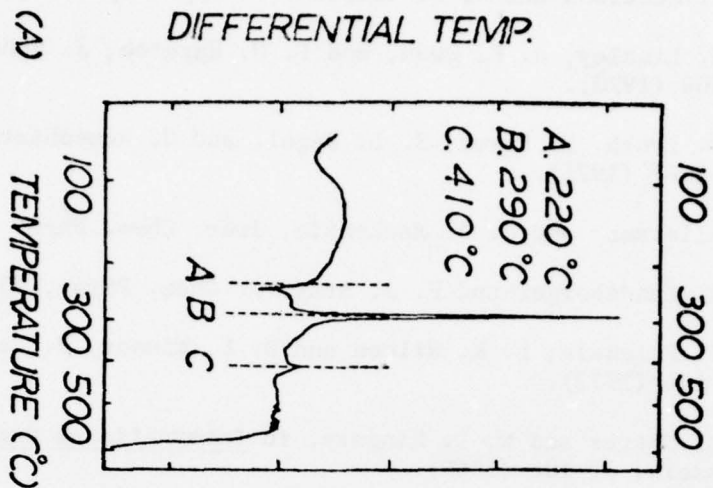


Figure 1. (A) typical DTA curve and (B) resulting heat treatment schedule for all  $V_2O_5$ -based glasses of this research. The separate 220°C temperature was found necessary to allow some initial structural readjustment in the glasses prior to the onset of crystallization.

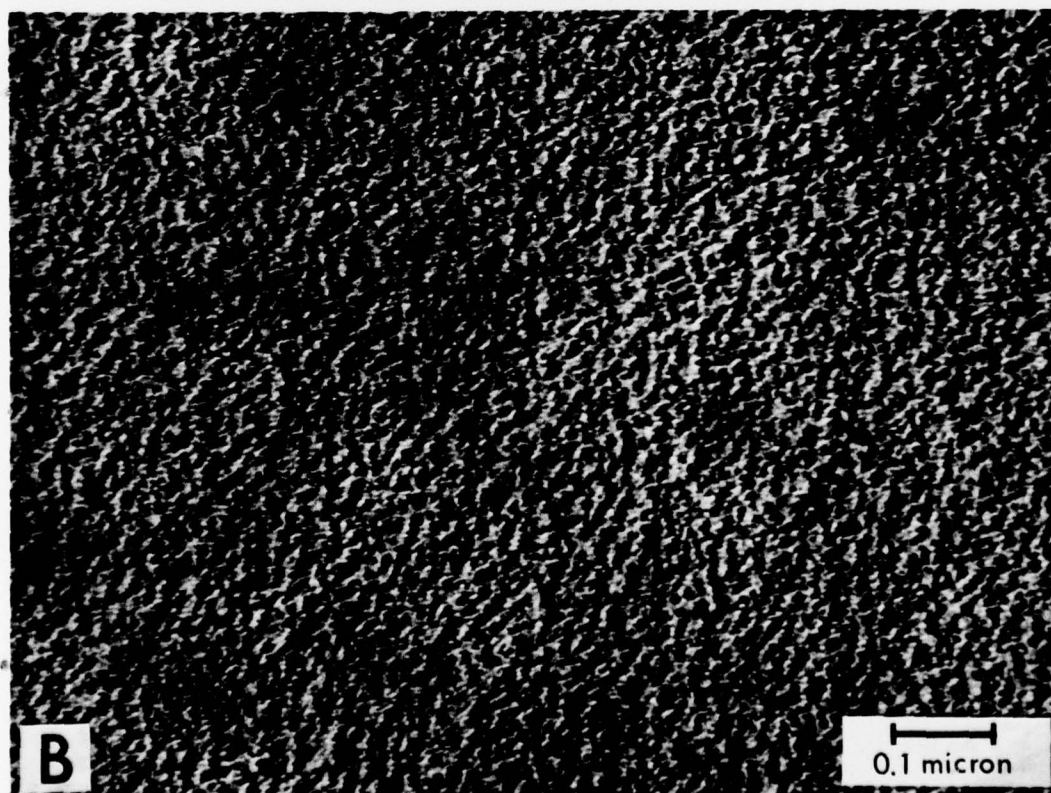
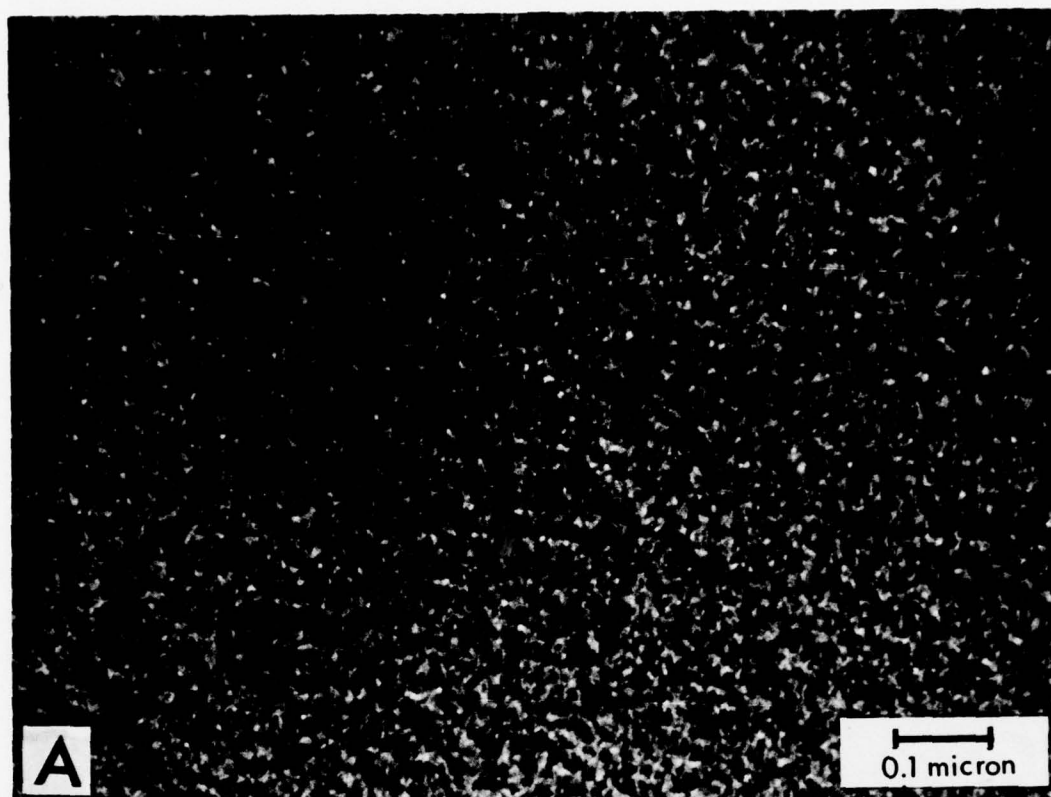


Figure 2. Replicate TEM micrographs showing progressive phase separation and crystallization in the 000 glass. (A) as cooled, (B) 220°C - 4 hrs. (bar = 0.5 $\mu$ m).



Figure 2. Replicate TEM micrographs showing progressive phase separation and crystallization in the 000 glasses. (C) 290°C - 6 hrs. and (D) 410°C - 6 hrs. (bar = 0.5 $\mu$ m).



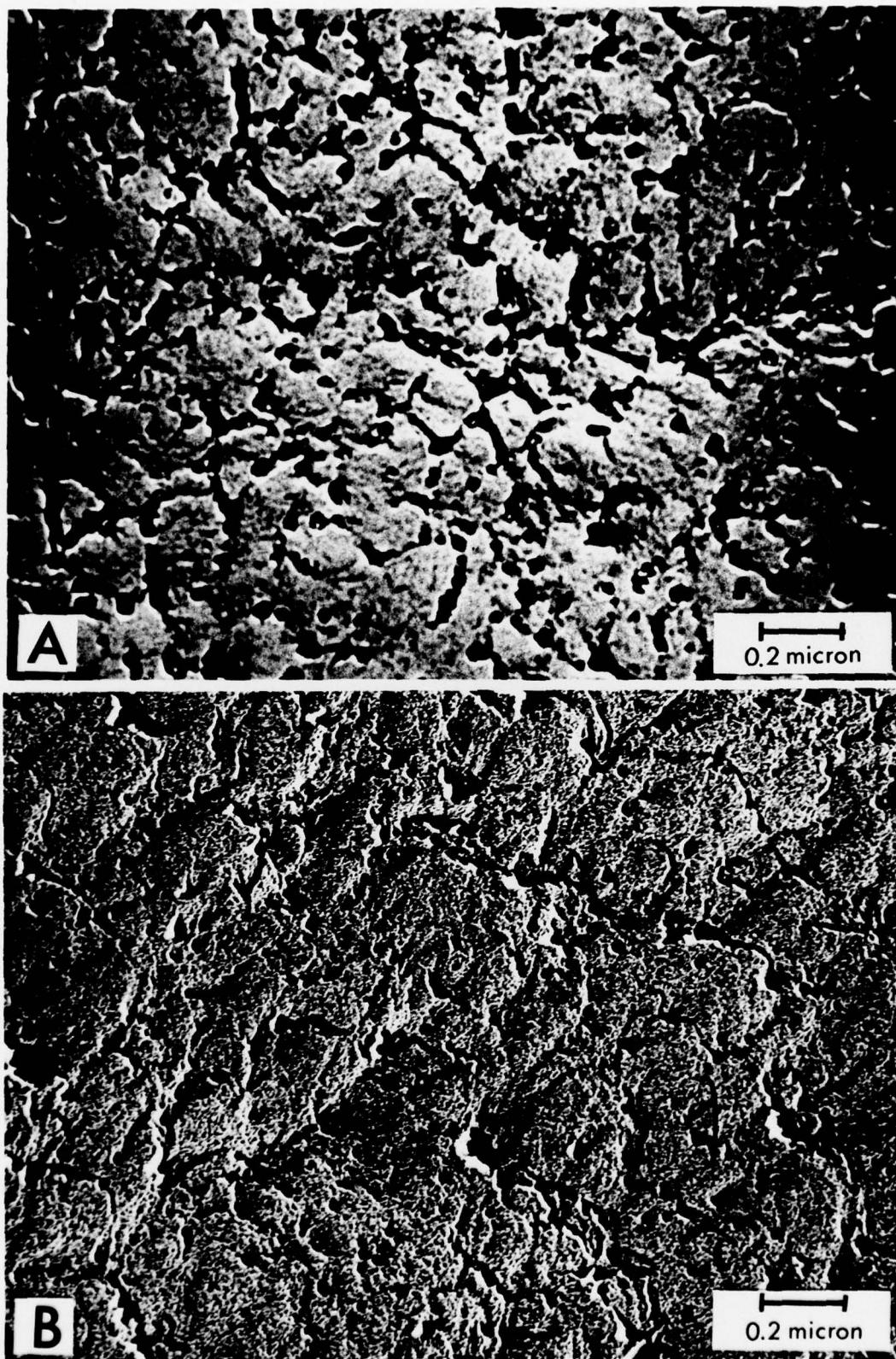


Figure 3. Replicate TEM micrographs, representative of all ternary compositions, showing crystallization in the 006 glass. (A) 290°C - 6 hrs. and (B) 410°C - 6 hrs. The microstructure of the as-cooled and annealed glasses are similar to those of Fig. 2(A),(B). (bar = 0.5 $\mu$ m)

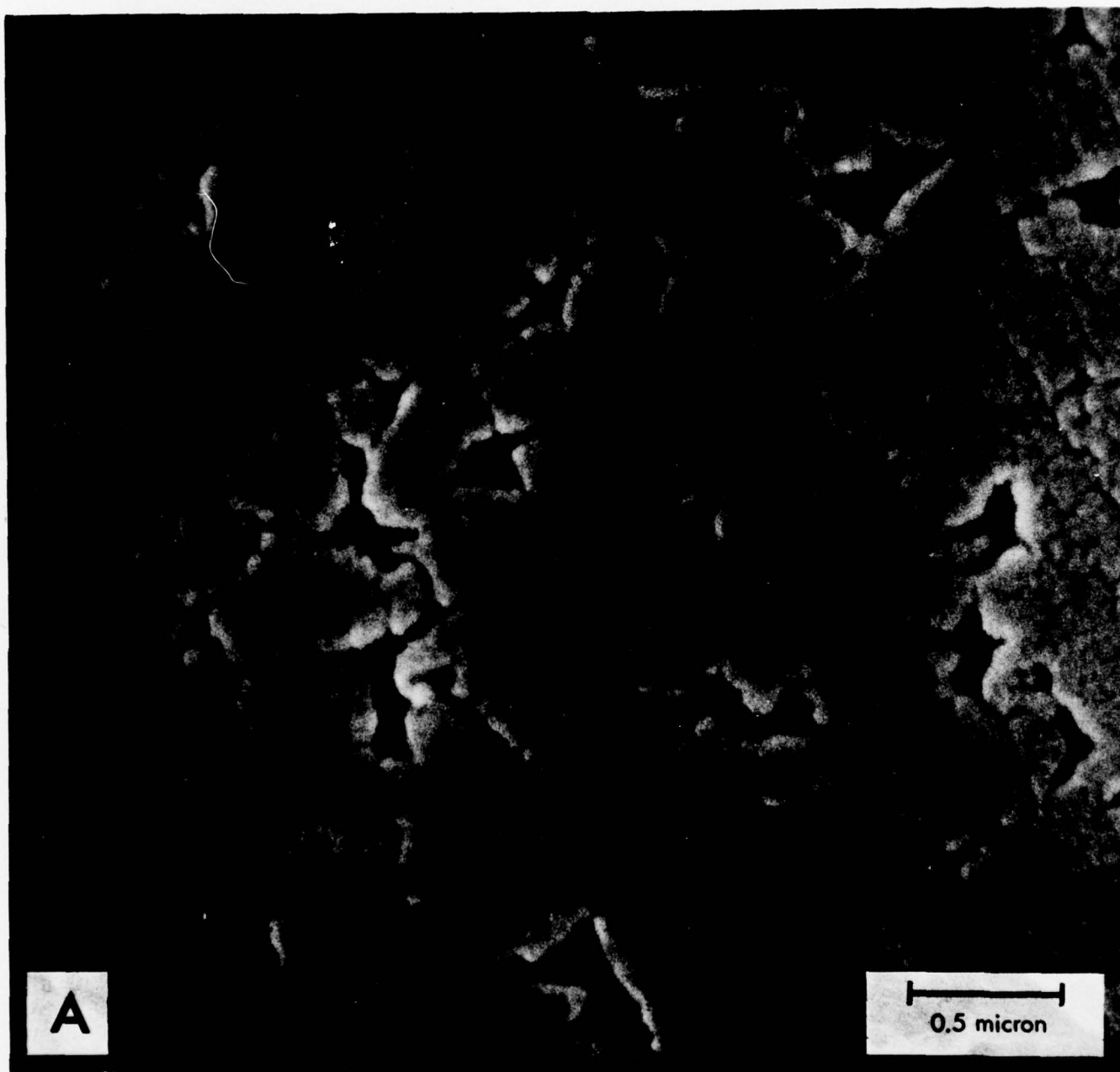


Figure 4 (A). SEM micrograph showing the polycrystalline  $V_2O_5$  in polished and etched surface of 000-290°C - 6 hrs., etched with  $H_2O$  for 90 sec. (bar =  $1\mu m$ )

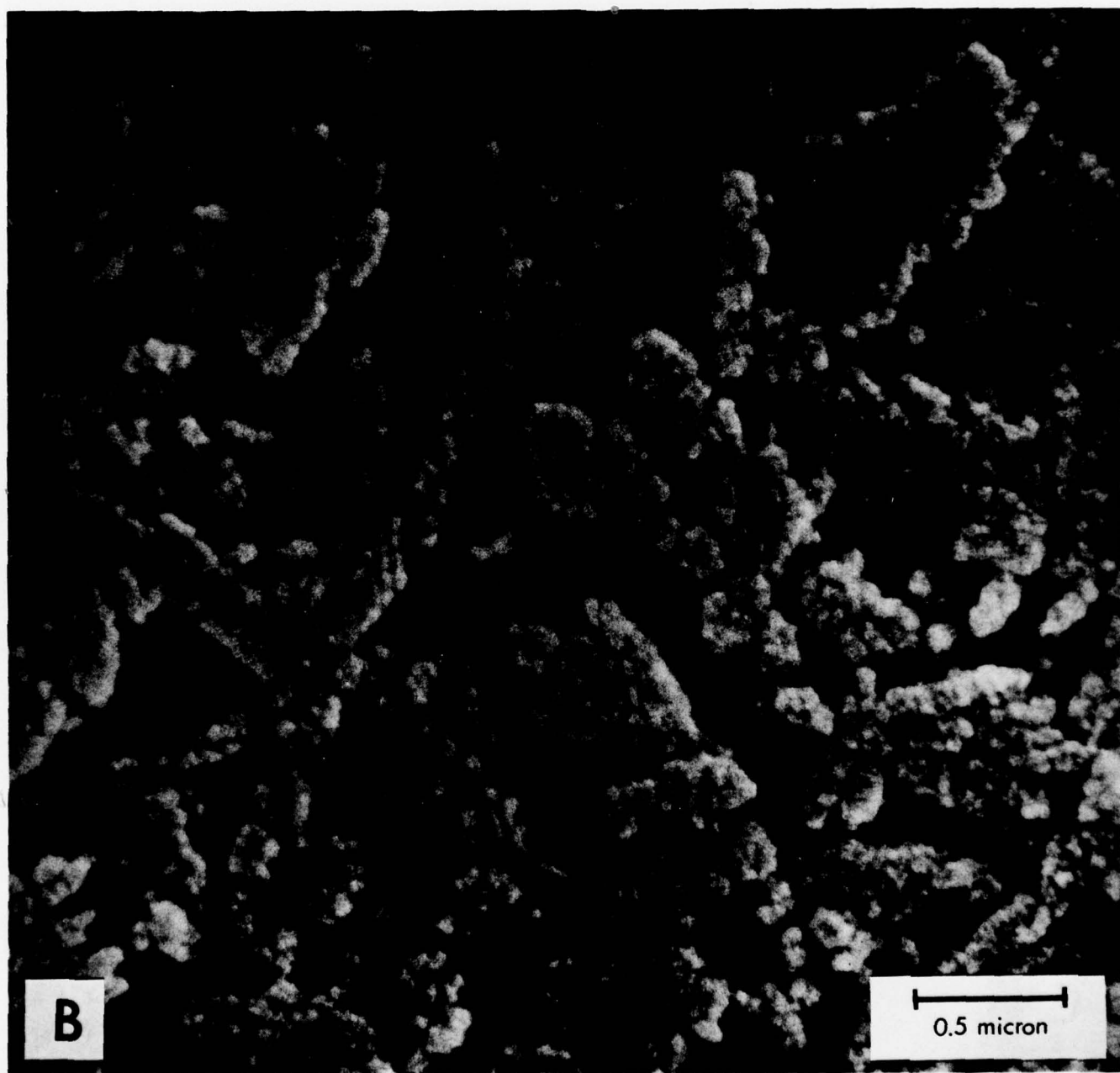


Figure 4 (B). SEM micrograph showing the polycrystalline  $V_2O_5$  in polished and etched surface of 000-290°C - 6 hrs., etched with 1% HCl for 50 sec. (bar = 1 $\mu$ m)

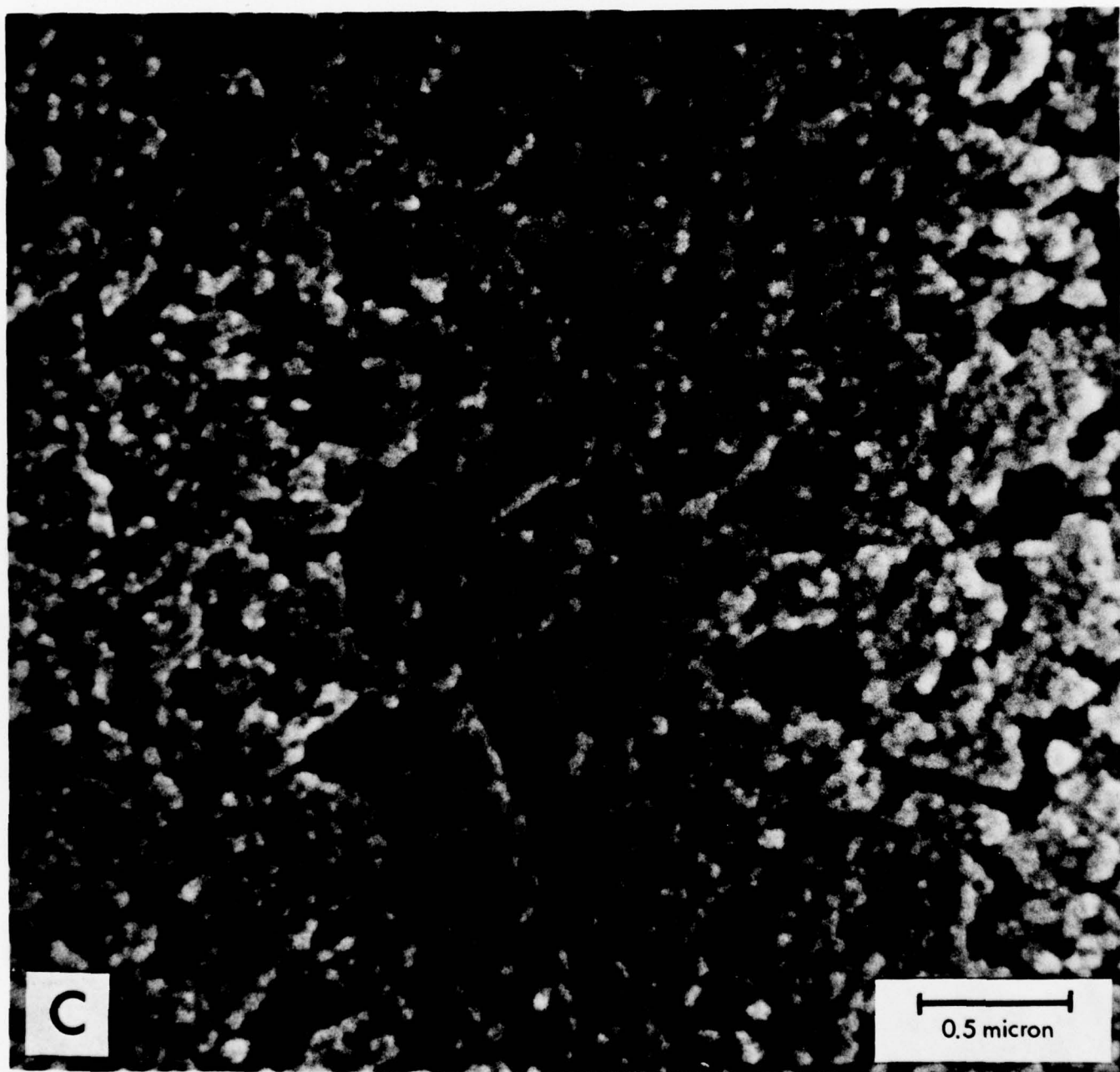


Figure 4 (C). SEM micrograph showing the polycrystalline  $V_2O_5$  in polished and etched surface of 000-410°C - 6 hrs., etched with 1% HCl for 50 sec. (bar = 1 $\mu$ m)



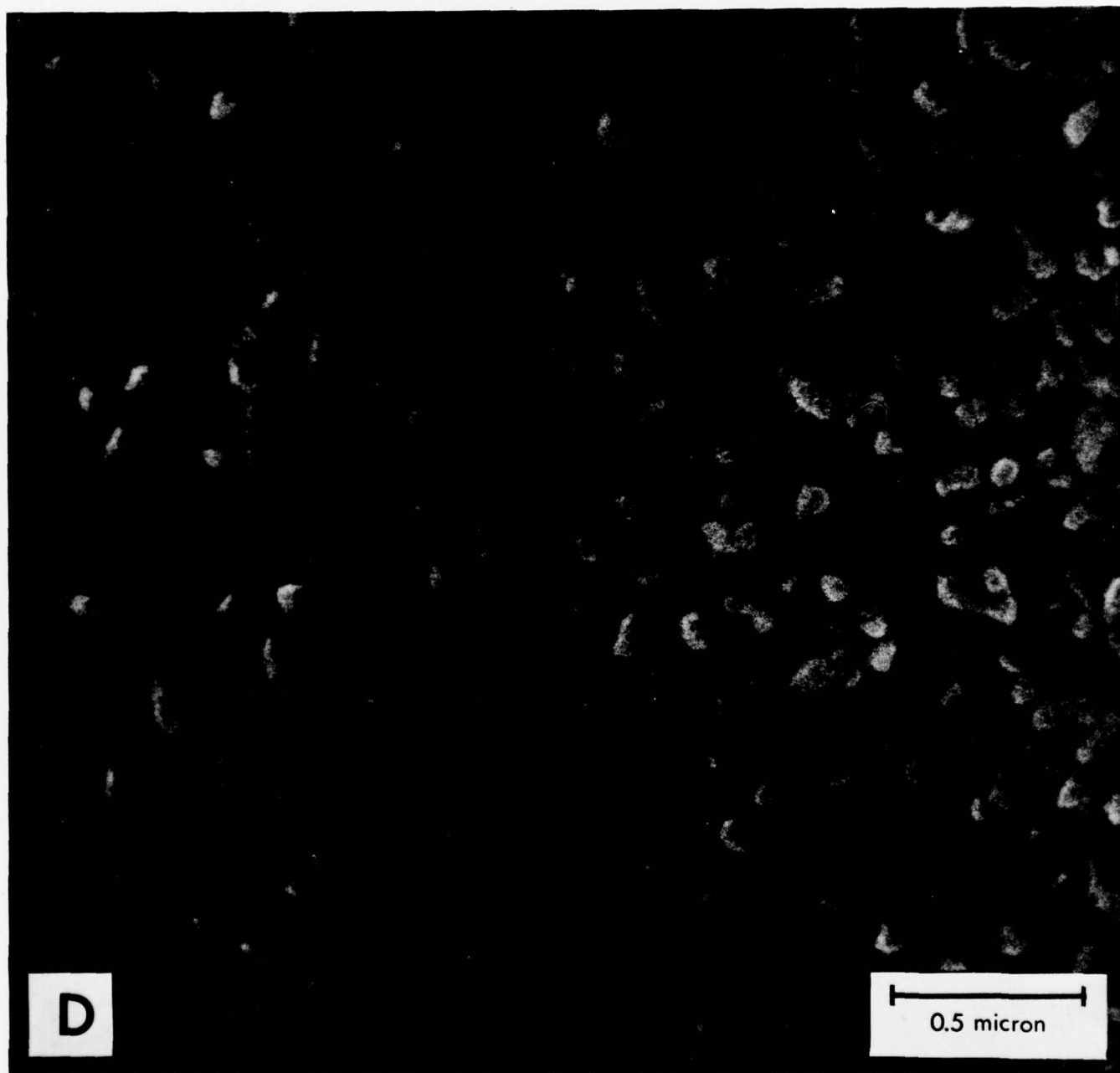


Figure 4 (D). SEM micrograph showing the polycrystalline  $V_2O_5$  in polished and etched surface of 006-290°C - 6 hrs., etched with 1% HCl for 50 sec. (bar = 1 $\mu$ m)

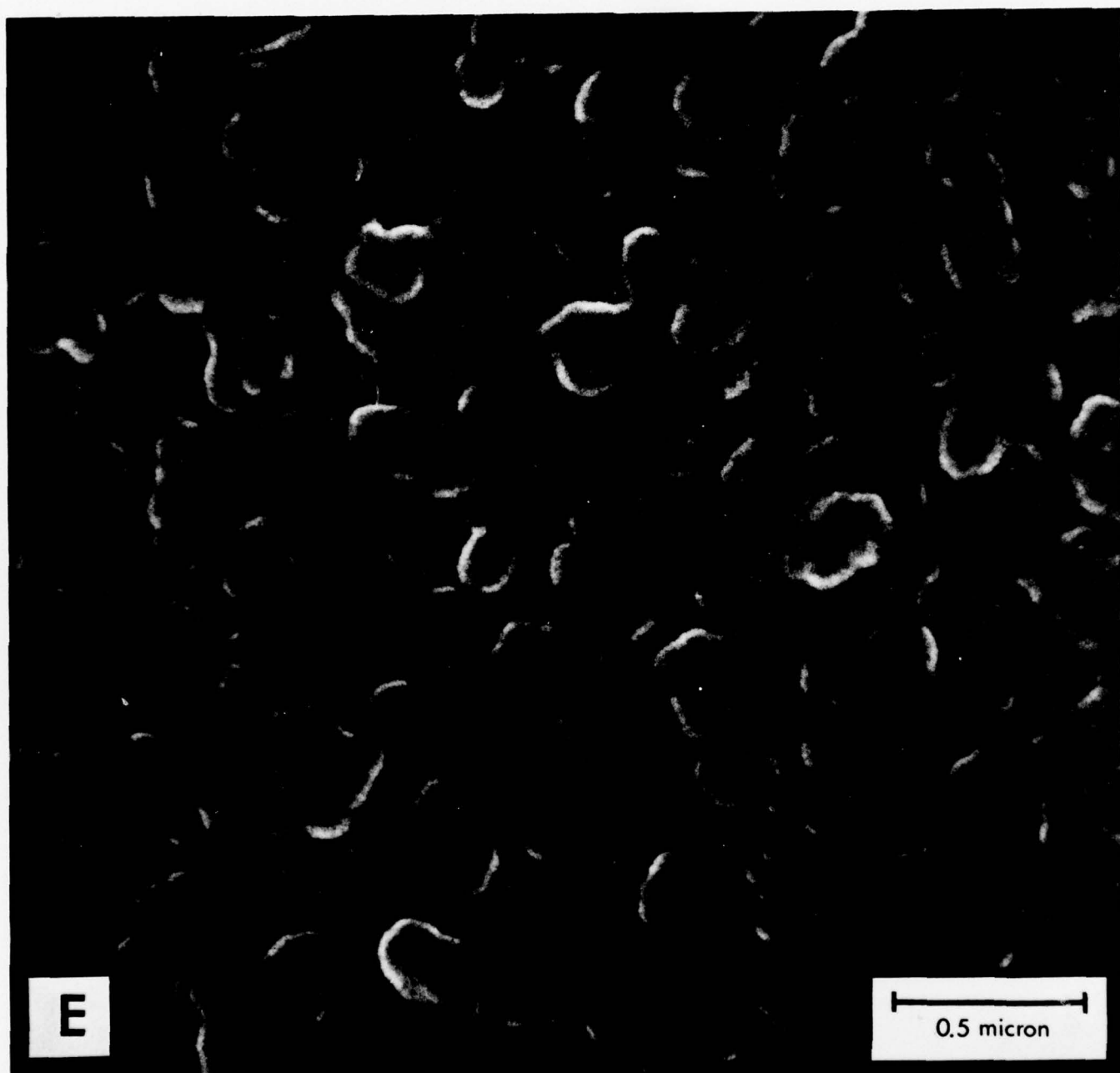


Figure 4 (E). SEM micrographs showing the polycrystalline  $V_2O_5$  in polished and etched surface of 006 -  $410^{\circ}C$  - 6 hrs., etched with 1% HCl for 50 sec. (bar =  $1\mu m$ )

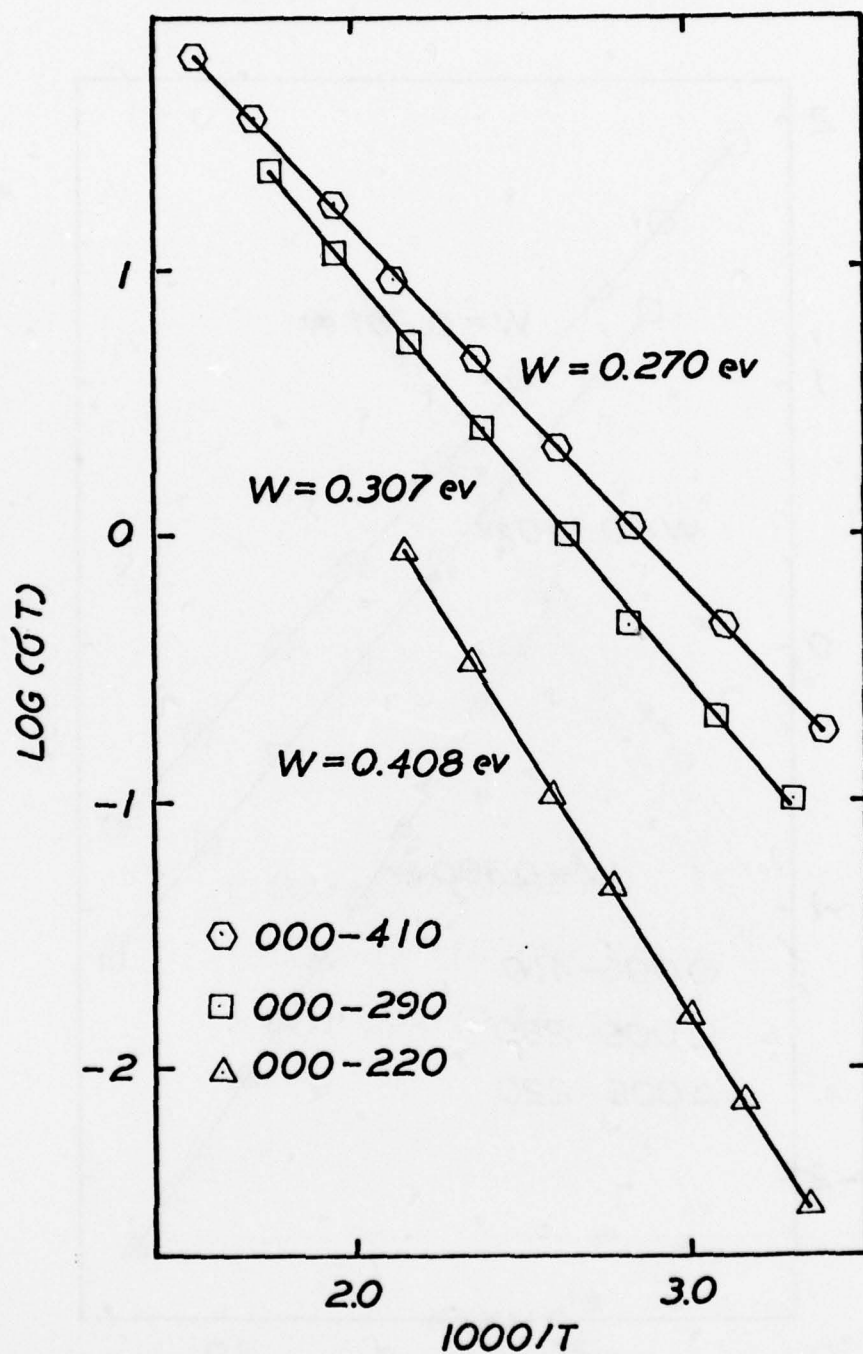


Figure 5 (A). Curves of  $\log \sigma$  vs.  $1/T$  showing the changes in conductivity as a function of the temperature of crystallization for composition 000.

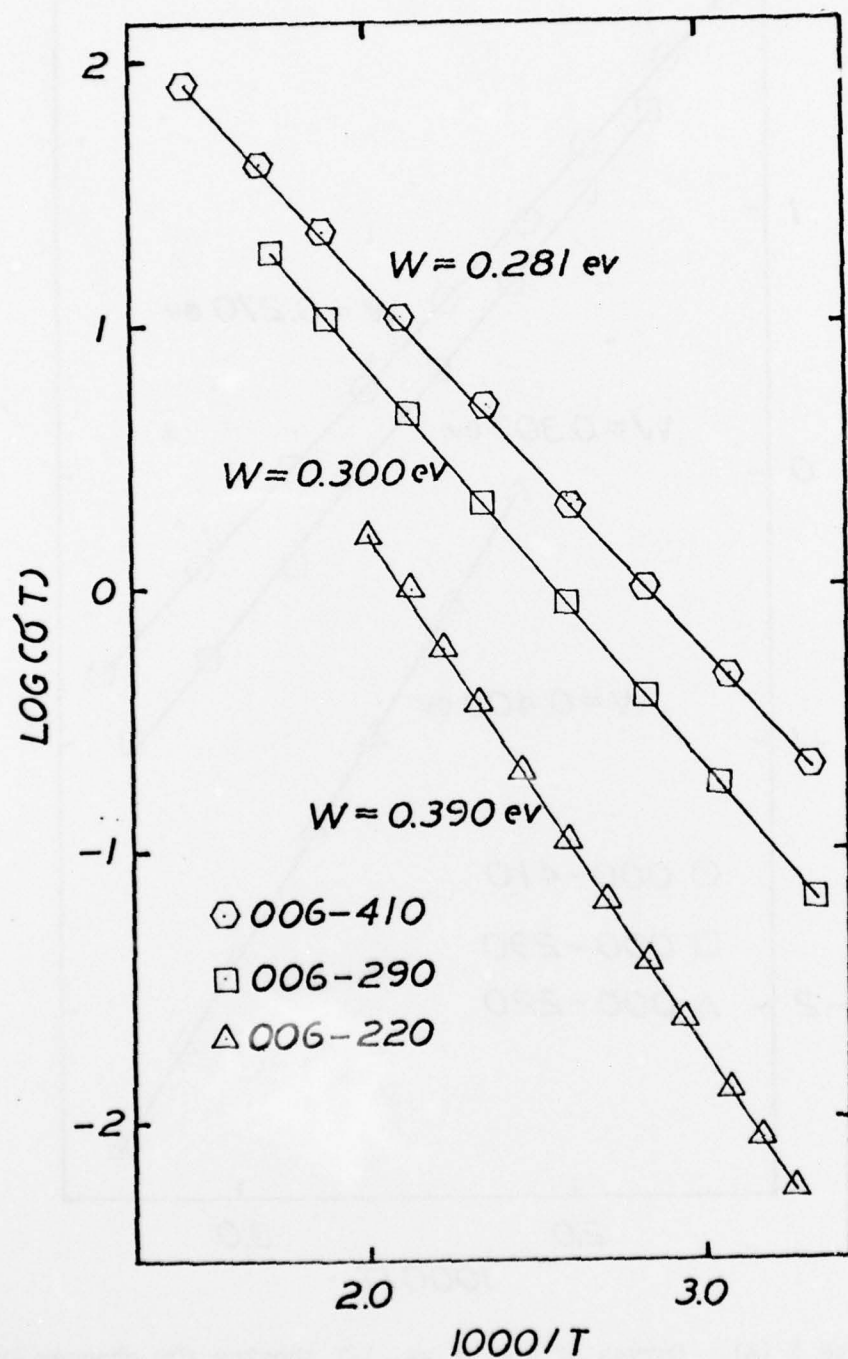


Figure 5 (B). Curves of  $\log \sigma T$  vs.  $1/T$  showing the changes in conductivity as a function of the temperature of crystallization for composition 006.



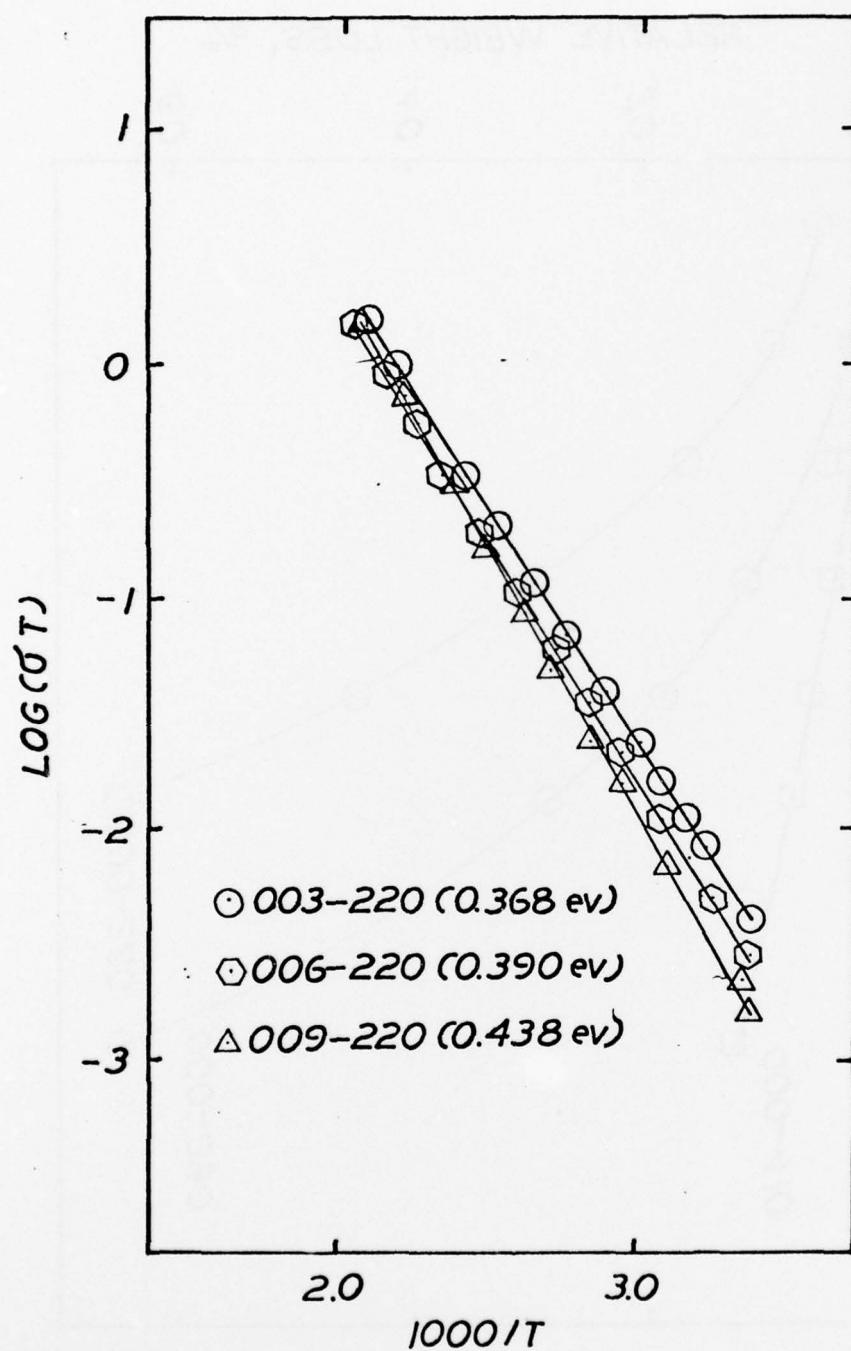


Figure 5 (C). Curves of  $\log \sigma T$  vs.  $1/T$  showing the changes in conductivity as a function of the temperature of crystallization as a function of the changing  $V_2O_5$  content in the glasses annealed at  $220^\circ\text{C}$ .

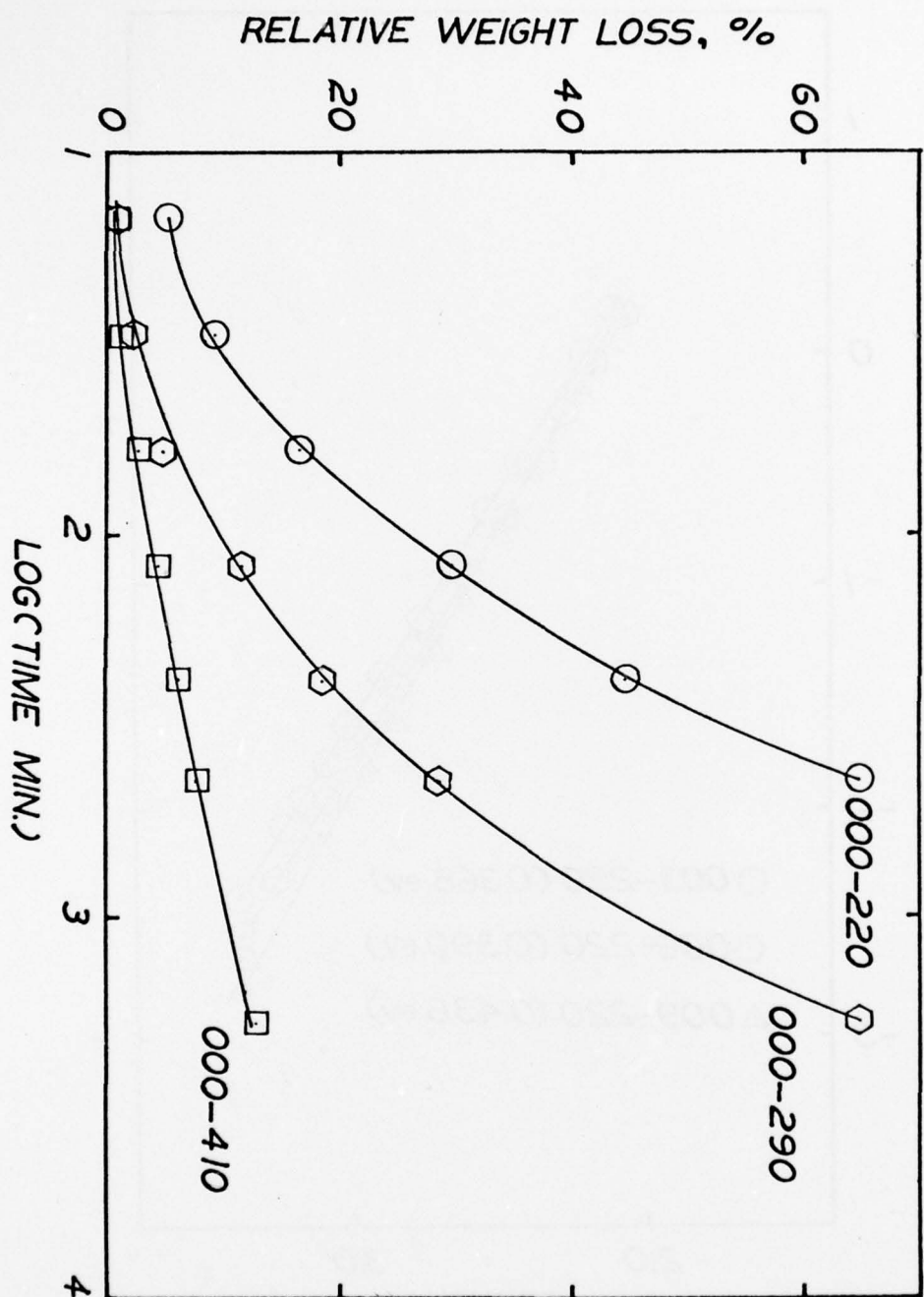


Figure 6(A). Curves of percentage weight loss of the annealed and progressively crystallized 000 glasses as a function of the log of time of immersion in static  $H_2O$ .

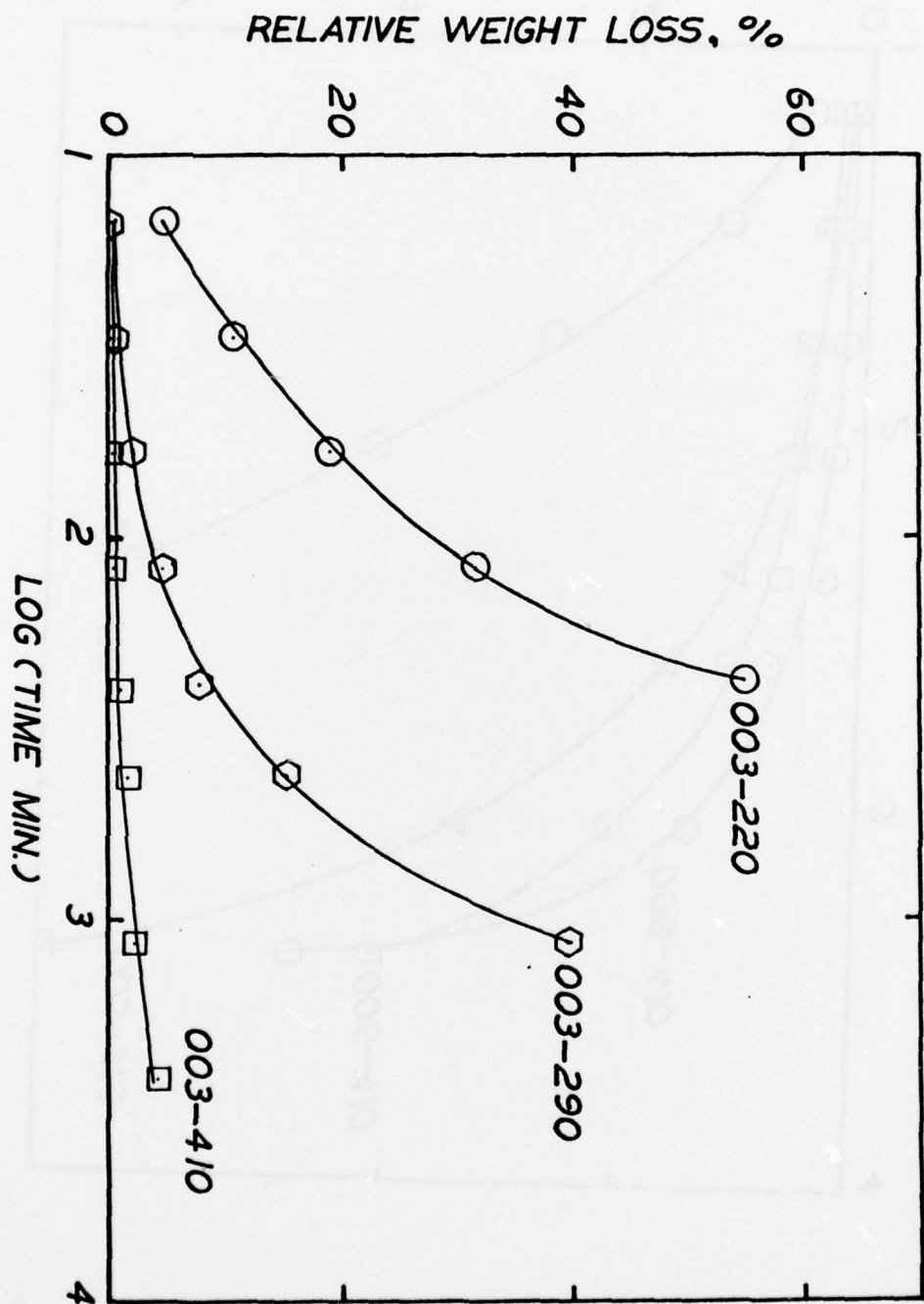


Figure 6 (B). Curves of percentage weight loss of the annealed and progressively crystallized 003 glasses as a function of the log of time of immersion in static  $H_2O$ .

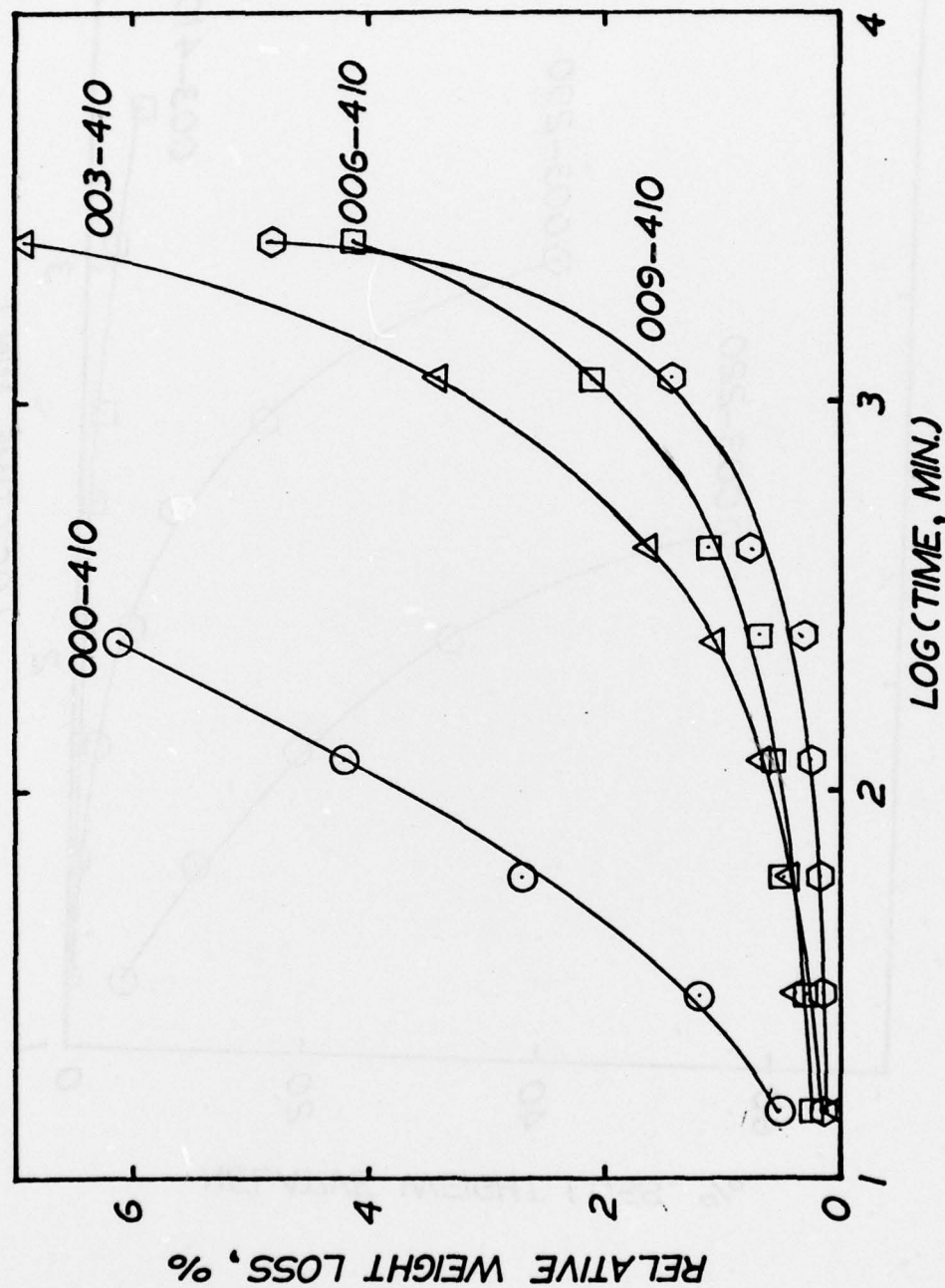


Figure 6 (Cl). Curves of percentage weight loss of the progressively crystallized glasses at 410°C as a function of the log of time of immersion in static H<sub>2</sub>O.